Neuroendocrinology Letters Volume 38 No. 1 2017
ISSN: 0172-780X; ISSN-L: 0172-780X; Electronic/Online ISSN: 2354-4716
Web of Knowledge / Web of Science: Neuroendocrinol Lett
Pub Med / Medline: Neuro Endocrinol Lett

ORIGINAL ARTICLE

Autophagy plays beneficial effect on diabetic encephalopathy in type 2 diabetes: studies *in vivo* and *in vitro*

Yu-Hong Jing [1,2], Lang Zhang [1], Li-Ping Gao [3], Chu-Chu Qi [1], Dan-Dan Lv [1,4], Yan-Feng Song [1], Jie Yin [1], De-Gui Wang [1],

1 Institute of Anatomy and Histology & Embryology, Neuroscience, School of Basic Medical Sciences, Lanzhou University, Lanzhou, P. R. China
2 Key Laboratory of Preclinical Study for New Drugs of Gansu Province, Lanzhou University, Lanzhou, P. R. China
3 Institute of Biochemistry and Molecular Biology, School of Basic Medical Sciences, Lanzhou University, Lanzhou, P. R. China
4 Department of Gastroenterology, Tangdu Hospital, Fourth Military Medical University, Xi'an, Shanxi Province, P. R. China

Correspondence to: Yu-Hong Jing, PhD.
Institute of Anatomy and Histology & Embryology
Neuroscience, School of Basic Medical Sciences
Key Laboratory of Preclinical Study for New Drugs of Gansu Province
Lanzhou University, Lanzhou, P.R. China.
E-MAIL: jingyh@lzu.edu.cn

Submitted: 2016-07-02 Accepted: 2016-11-23 Published online: 2017-02-27

Key words: **autophagy; T2DM; hypothalamus; lipotoxicity**

Neuroendocrinol Lett 2017; **38**(1):27–37 **PMID:** 28456145 NEL380117A02 • **www.nel.edu**

Abstract

OBJECTIVES: The hypothalamus regulates metabolism and feeding behavior by perceiving the levels of peripheral insulin. However, little is known about the hypothalamic changes after aberrant metabolism. In this study, we investigated the changes of insulin and autophagy relevant signals of hypothalamus under diabetes mellitus.

METHODS: C57B/L mice were injected with low-dose streptozotocin (STZ) and fed with high-fat diet to induce type 2 diabetes mellitus. *In vitro*, PC12 cells were treated with oleic acid to mimic lipotoxicity.

RESULTS: Results showed that the cholesterol level in the hypothalamus of the diabetic mice was higher than that of the normal mice. The expression of insulin receptors and insulin receptor substrate-1 were downregulated and the number of Fluoro-Jade C positive cells significantly increased in the hypothalamic arcuate nucleus of the diabetic mice. Furthermore, Upregulation of mammalian target of rapamycin (mTOR) and downregulation of LC 3II were obvious in the hypothalamus of the diabetic mice. *In vitro*, results showed that high-lipid caused PC12 cell damage and upregulated LC3 II expression. Pretreatment of cells with 3-methyladenine evidently downregulated LC3 II expression and aggravated PC12 cell death under high lipid conditions. By contrast, pretreatment of cells with rapamycin upregulated LC3 II expression and ameliorated PC12 cell death caused by lipotoxicity.

CONCLUSION: These results demonstrate that autophagy activation confers protection to neurons under aberrant metabolism and that autophagy dysfunction in the hypothalamus occurs in the chronic metabolic disorder such as T2DM.

INTRODUCTION

Autophagy is a conserved self-degradation process in eukaryotes that can selectively degrade cellular components, including long-lived proteins, misfolded protein, and aged organelles (Mizushima, 2005). Autophagy involves multi-steps including autophagosome formation, autophagosome-lysosome fusion, and intra-autophagosomal content degradation by lysosomal hydrolases (Osellame & Duchen 2014). Autophagy is strictly controlled by signal molecules, such as mammalian target of rapamycin (mTOR), ATG-associated proteins, and PI_3K (O'Farrell *et al.* 2013; Maiese 2015 2016). Rapamycin and 3-MA regulate autophagy by inhibiting mTOR and PI_3K, respectively (Rubinsztein *et al.* 2007; Yang *et al.* 2008). Recent evidence has suggested that autophagy has a dual function in neurodegenerative diseases (Liu *et al.* 2015b). Autophagy elicits either protective or detrimental effects on neurodegenerative diseases depending on the environment (Tung *et al.* 2012). Sustained activation of autophagy by infection or energy deficiency leads to autophagic cell death. Alternatively, autophagy declines in the presence of neurodegenerative diseases, such as Alzheimer's disease (AD), Parkinson's disease, and Huntington's disease (Ling & Salvaterra 2009). In the early stage of neurodegenerative diseases, autophagy activation accelerates the elimination of denatured protein, thereby blocking further disease development. However, the capacity of autophagy to degrade aggregated proteins is weakened when autophagy reaches a certain saturation point during development of neurodegeneration. Seriously, autophagy may also become defective in neurodegeneration.

Type 2 diabetes mellitus (T2DM) is characterized by insulin resistance and is usually coupled with obesity and aberrant lipid metabolism (Savage *et al.* 2007). A recent study has reported that T2DM affects the central nervous system (CNS) by causing cognition impairment (Biessels and Reagan, 2015). Furthermore, emerging data have indicated that T2DM is closely linked to AD onset. Epidemiological studies have found that T2DM and insulin resistance can double the risk of developing AD (Haan, 2006; Li and Holscher, 2007). Neuroimaging examination has revealed the presence of brain atrophy in diabetic patients (Lee *et al.* 2014). Recent research has proven that insulin has important functions in the CNS and that insulin receptors (IRs) are abundant in brain areas, including the hippocampus, olfactory bulb, cortex, and hypothalamus (Gray *et al.* 2014). Insulin generated from pancreatic islets can cross the blood brain barrier. Diabetes mellitus is characterized by insulin deficiency or insulin resistance, which may affect CNS. Accumulating evidence indicated that impairments in cerebral glucose utilization and energy metabolism represent very early abnormalities that precede or accompany the initial stages of cognitive impairment (Iwangoff *et al.* 1980; Sims *et al.* 1980; Hoyer, 2004). Because insulin signaling impaired has an important role in the pathogenesis of AD, recently, researchers named AD as "type 3 diabetes" (Steen *et al.* 2005). Insulin resistance in T2DM is partly mediated by reduced insulin receptor expression, insulin receptor tyrosine kinase activity, insulin receptor substrate (IRS) type 1 expression, and/or phosphatidyl-inositol-3 (PI3) kinase activation in skeletal muscle and adipocytes (Bernal-Reyes, 2012).Type 3 diabetes mellitus corresponds to a chronic insulin resistance plus insulin deficiency state that is largely confined to the brain but, can overlap with T2DM. Several studies have been suggested that T3DM represented a major pathogenic mechanism of AD neurodegeneration (Rivera *et al.* 2005; Steen *et al.* 2005).

Abnormal glucose and lipid metabolism caused by T2DM can influence animal feeding behavior and energy balance, both of which are regulated by the hypothalamus. Therefore, we hypothesized that diabetes mellitus affects the CNS, especially neuroendocrine-related brain areas, hypothalamus. Insulin signals trigger PI3K activation and modify mTOR activation to negatively regulate autophagy associated signals. Therefore, this study evaluated neurodegeneration and examined insulin and autophagy associated signals in the hypothalamus of T2DM mice. The response of PC12 cells to autophagy inhibition or activation under high-lipid conditions was analyzed to verify the roles of autophagy in neurodegeneration induced by the metabolic disorder.

MATERIALS AND METHODS

Animal preparation

Fifty 6- to 8-week-old male C57B/L mice weighing 22±2 g were purchased from the Laboratory Animal Center of Lanzhou University (Lanzhou, China). All mice were housed under controlled temperature (23±2 °C) and humidity (40% to 60%) with natural light. All experimental manipulations were undertaken in accordance with the Institutional Guidelines for the Care and Use of Laboratory Animals. Basic feed component contained 5% fat, 53% carbohydrates, and 23% protein, which produced 25 kJ/kg of total energy. High-fat diet contained the following: 22% fat, 48% carbohydrates, and 20% protein, which produced 44.3 kJ/kg of total energy.

Reagents

Streptozotocin (STZ), rapamycin, 3-MA, monodansylcadaverine (MDC), propidium iodide (PI), and LC3 antibody were purchased from Sigma (St. Louis, MO, USA). Antibodies against IR, insulin receptor substrate-1 (IRs1), mTOR, and phosphorylated mTOR were obtained from Santa Cruz (Santa Cruz, CA, USA). Fluoro-Jade C (FJC), GAPDH antibody, and electrochemiluminescent (ECL) reagents were obtained from Millipore (Bellerica, MA, USA). Detection kits for evaluating the levels of glucose, triglyceride, and choles-

terol were obtained from BiosinoBio-Technology and Science INC (Beijing, China).

Establishment of animal model

Male C57B/L mice were intraperitoneally injected with STZ (40 mg/kg body weight) dissolved in 50 mM citrate buffer (pH 4.5) for four consecutive days (once a day) to induce hyperglycemia, whereas control mice were injected with 50 mM citrate buffer. The induction of diabetes was confirmed after 7 d by measuring blood glucose levels using a glucose test kit. Animals with blood glucose levels above 250 mg/dL were fed with high-fat diet at indicated time points.

Blood parameter analysis

Plasma glucose, triglyceride, and cholesterol were measured using respective Enzymatic Diagnostic Kits. All data were obtained from two independent measurements, each with triplicate incubations.

Glucose tolerance test and insulin sensitivity test

For the glucose tolerance test and insulin sensitivity test, the mice fed with high-fat diet for 2 months were intraperitoneally injected with glucose (2 g/kg) or subcutaneously injected with human regular insulin (0.75 units/kg) after 12 h of fasting, respectively. Blood samples were collected from the tail vein at different time points. Blood glucose levels were measured as described above.

Cholesterol levels in the hypothalamus

Diabetic mice at 4 months of age (n=6) were selected to measure cholesterol levels in the hypothalamus. The mice were anaesthetized with chloral hydrate and perfused with ice-cold 0.9% saline through the heart. Brains of the mice were removed and kept on ice. Then the hypothalamus was dissected and the total protein was extracted using lysis buffer (20 mM Tris-HCl, pH 8; 1% Triton X-100; 137 mM NaCl; 1.5 mM $MgCl_2$; 10% glycerol; 1 mM EGTA; 10 mM β-glycerophosphate; 1 mM PMSF; 1 μg/mL leupeptin; 1 μg/mL aprotinin). The total cholesterol levels in the hypothalamus were measured using the Amplex Red Cholesterol Assay Kit (Invitrogen, USA) according to the previous study (Zhang *et al.* 2015). Briefly, brain tissue proteins were suspended in 1x cholesterol reaction buffer (0.1 M potassium phosphate, pH 7.4, 0.05 M NaCl, 5 mM cholic acid, and 0.1% Triton X-100). Subsequently, 50 μL of 150 μM Amplex Red reagent (1 U/mL horseradish peroxidase, 1 U/mL cholesterol oxidase, and 1 U/mL cholesterol esterase) was added to 50μL samples in 96-well plates. After incubation for 60 min at 37 °C in the dark, sample fluorescence was measured using a microplate reader (Tecan, Switzerland) at 530 nm (excitation) and 590 nm (emission). The total cholesterol (TC) content was determined by measuring the cholesterol concentration following digestion with cholesterol esterase (CE). To measure free cholesterol (FC), CE was omitted from the assay. Each sample was analyzed in triplicate, and at least three independent experiments were performed. Values were obtained from a cholesterol standard curve and then normalized.

FJC staining

Diabetic mice at 4 months (n=6) were selected to assess neuron degeneration in the hypothalamus. The mice were subjected to cardiac perfusion with 0.9% normal saline followed by 0.1 mol/L phosphate buffer with 4% paraformaldehyde. The brains of the mice were removed and post fixed in 4% paraformaldehyde overnight, and then sequentially dehydrated in 20% and 30% sucrose solutions in 0.1 mol/L phosphate buffer (pH 7.4) until they sank. The brains were sectioned in the coronal plane at 30 μm thickness using a freezing microtome. Six sections at –2.2 mm to –4.6 mm from the bregma (at 400 μm intervals) were selected. FJC staining and imaging analyzing were performed as previously described. Dried sections were dipped in 80% ethanol solution that contains 1% sodium hydroxide, 70% ethanol, and 0.06% potassium permanganate for 5, 2, and 10 min, respectively. The sections were rinsed with distilled water and then incubated with 0.0004% FJC in 0.1% acetic acid for 20 min. FJC staining was visualized under a fluorescent microscope at 480 nm excitations and 525 nm emissions. Images were acquired through a 20× objective, and the number of FJC-positive cells in the hypothalamus was counted. The total number of positive cells in the hippocampus and hypothalamus was calculated as $[(S1 + S2)/2 + (S2 + S3)/2 + (S3 + S4)/2 + (S4 + S5)/2 + (S5 + S6)/2] \times 10$, where S1 to S6 represent the number of cells in sections 1 to 6, respectively.

Neuron autophagy of the hypothalamic arcuate nucleus under an electron microscope

Diabetic mice at 4 months (n=3) were perfused and fixed. The brains of the mice were sectioned in the coronal plane at 500 μm thickness, and the arcuate nucleus was dissected under the microscope. The arcuate nucleus was fixed with 3% glutaraldehyde in phosphate buffer, post fixed with 2% osmium tetroxide, and then dehydrated with ethanol and acetone. The samples were embedded with Epon 812, polymerized at 72 °C for 48 h, and then cut into ultrathin sections (50 nm). The sections were placed on uncoated copper grids and then stained with 3% lead citrate-uranyl acetate. Images were examined under an electron microscope.

Western blot analysis

After the designated treatments, the hypothalamus of the diabetic mice or PC12 cells was lysed in lysis buffer (20 mM Tris–HCl, pH 8, 1% Triton X-100, 137 mM NaCl, 1.5 mM $MgCl_2$, 10% glycerol, 1 mM EGTA, 1 mM NaF, 1 mM Na_3VO_4, 10 mM β-glycerophosphate, 1 mM phenylmethylsulfonyl fluoride, 1 μg/mL leupeptin, 1 μg/mL aprotinin). Equal amounts of protein were separated by sodium dodecyl sulfate–polyacrylamide gel

electrophoresis and then transferred onto membranes. The membranes were incubated overnight with primary antibodies against IR-β (1:1000), IRs1 (1:1000), LC3 (1:5000), mTOR (1:1000), phospho-mTOR (1:1000), and GAPDH (1:5000). The membranes were washed, incubated with horseradish peroxidase-conjugated secondary antibody, and then visualized by an ECL substrate. Bands were then quantified using ImageJ software.

Cell culture and treatment

PC12 cells were cultured in Dulbecco's modified Eagle's medium (supplemented with 10% fetal calf serum, 2 mM glutamine, 100 units/mL penicillin, and 100 μg/mL streptomycin) at 37 °C in a humidified atmosphere of 5% CO2. The cells were pretreated with or without 2.5 mM 3-MA or 2 μM rapamycin for 2 h and then treated with 300 μM oleic acid for 24 h.

MDC incorporation assay

MDC is a fluorescent compound that can be used as a tracer for autophagic vacuoles. After the designated treatments, the PC12 cells were incubated with 50 μM MDC at 37 °C for 1 h and then with 5 μg/mL PI at 37 °C for 10 min. Thereafter, the cells were washed once with PBS and then observed under a fluorescence microscope. Ten visual fields were randomly selected and captured through a 20× objective. The number of positive cells was counted in each view.

Statistical analysis

Results of the *in vivo* and *in vitro* experiments are presented as mean ± SEM and mean ± SD, respectively. Data were analyzed by two-way ANOVA and t-test. Statistical significance was considered at $p<0.05$.

RESULTS

Low-dose STZ combined with high-fat diet induced insulin resistance in C57B/L mice

Hyperglycemia (Figure 1A), hypertriglyceridemia (Figure 1B), and hypercholesterolemia (Figure 1C) were observed in the diabetic mice for four continuous months. In addition, the level of plasma cholesterol remained high. The results showed that the response rate to glucose (Figure 1D) and sensitivity to insulin (Figure 1E) of the diabetic mice decreased at 2 months after STZ injection combined with high-fat diet. These results suggested that the diabetic mice developed insulin resistance.

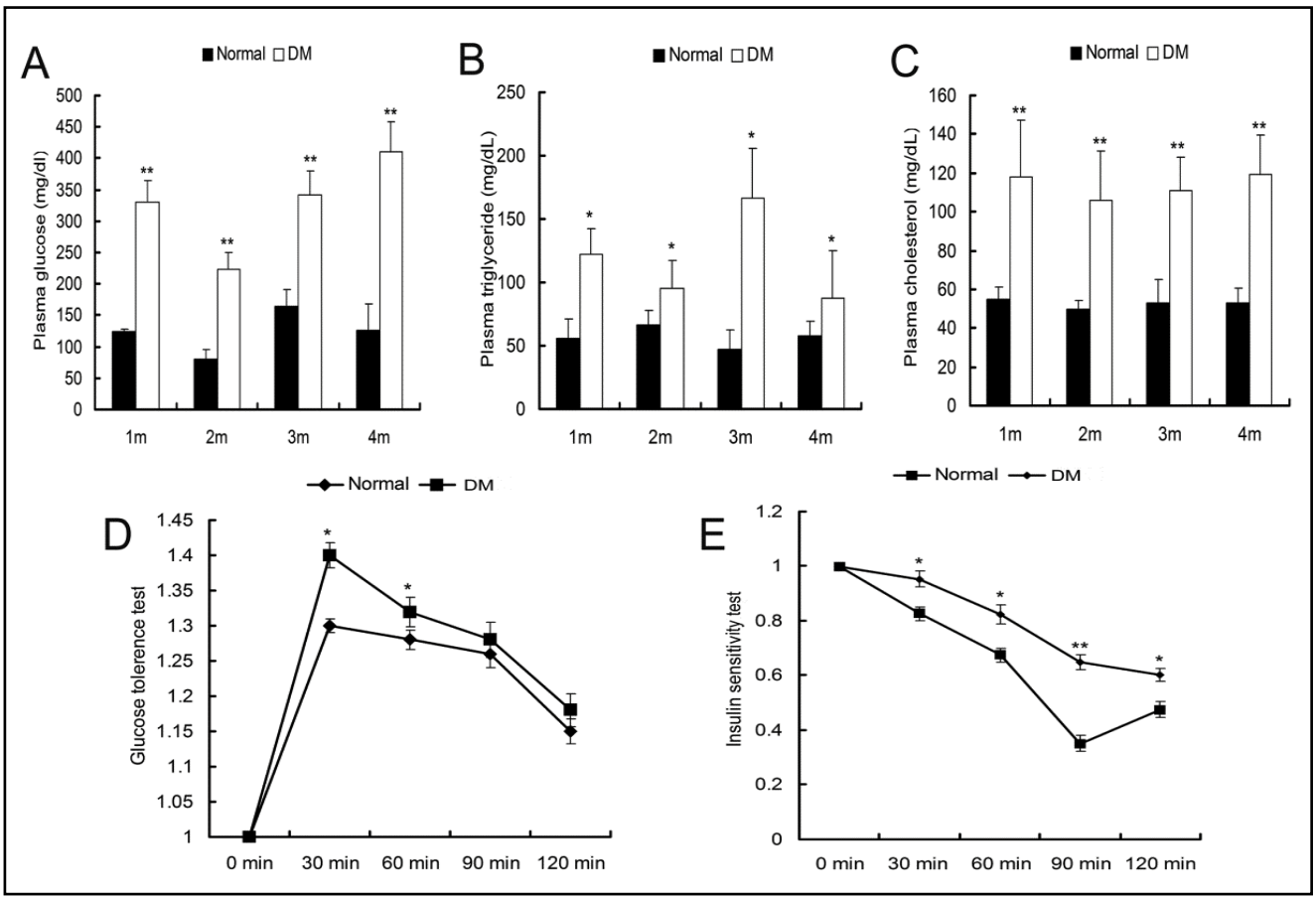

Fig. 1. Blood biochemistry analysis in C57B/L mice treated with low-dose STZ combined with high-fat diet. (A), blood glucose; (B), plasma triglyceride; (C), plasma cholesterol; (D), glucose tolerance test; and (E), insulin sensitivity test. Data are presented as mean ± SEM. n=20. * $p<0.05$, ** $p<0.01$, mice treated with low-dose STZ combined with high-fat diet at indicated time vs. normal mice.

Changes in cholesterol content and insulin signals in the hypothalamus of T2DM mice

As shown in Figure 2A, the cholesterol level in the brain tissues of the diabetic mice was significantly higher than that of the normal mice at 4 months after STZ injection combined with high-fat diet. The protein expression levels of IR-β and IRs1 in the hypothalamus decreased in the T2DM mice compared with the normal mice (Figures 2B, C and D). These findings suggested that peripheral metabolic disturbance in the T2DM mice altered the cholesterol level and insulin signals in the hypothalamus.

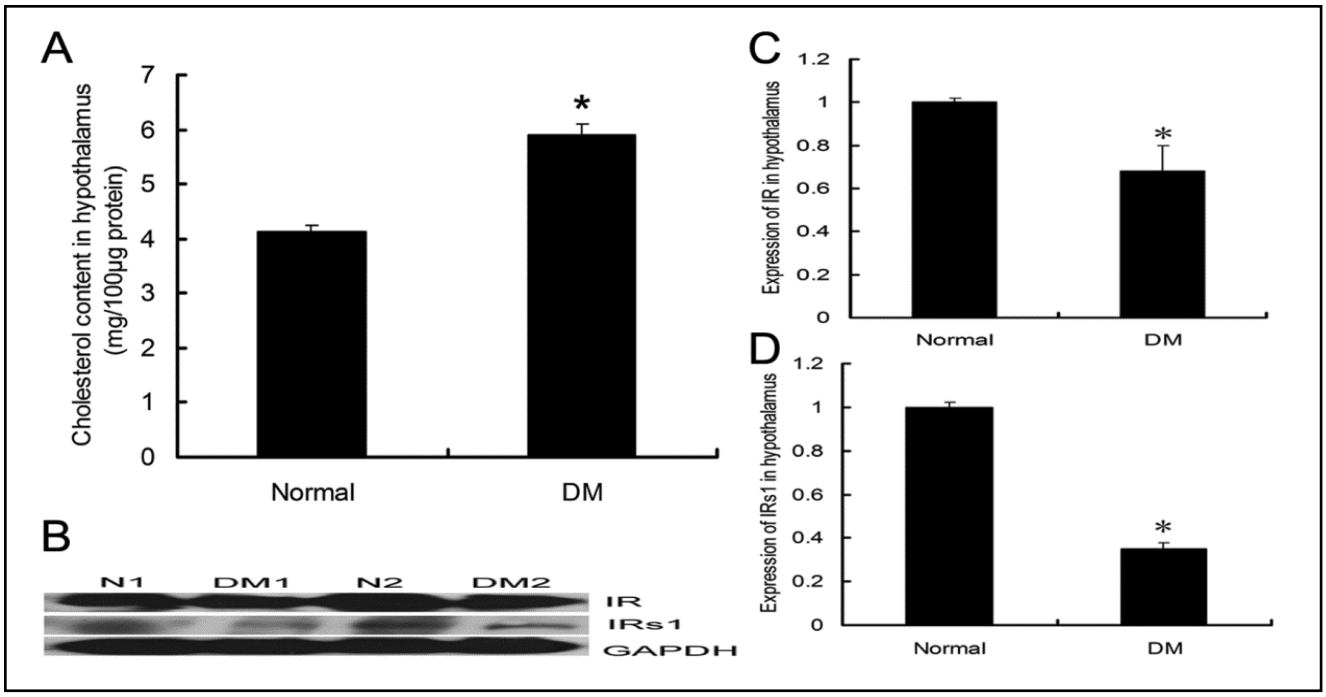

Fig. 2. Changes in cholesterol content and insulin signals in the hypothalamus of T2DM mice. (A), cholesterol content analysis in the hypothalamus. Data are presented as mean ± SEM. n=6. * $p<0.05$, mice treated with low-dose STZ combined with high-fat diet for 4 months vs. untreated mice. (B), protein expression levels of IR and IRs1 in the hypothalamus were analyzed by western blot. The blot shown here is representative of five experiments. (C and D), quantification of the protein expression levels of IR and IRs1. Data are presented as mean ± SEM. n=5. * $p<0.05$, mice treated with low-dose STZ combined with high-fat diet for 4 months vs. normal mice.

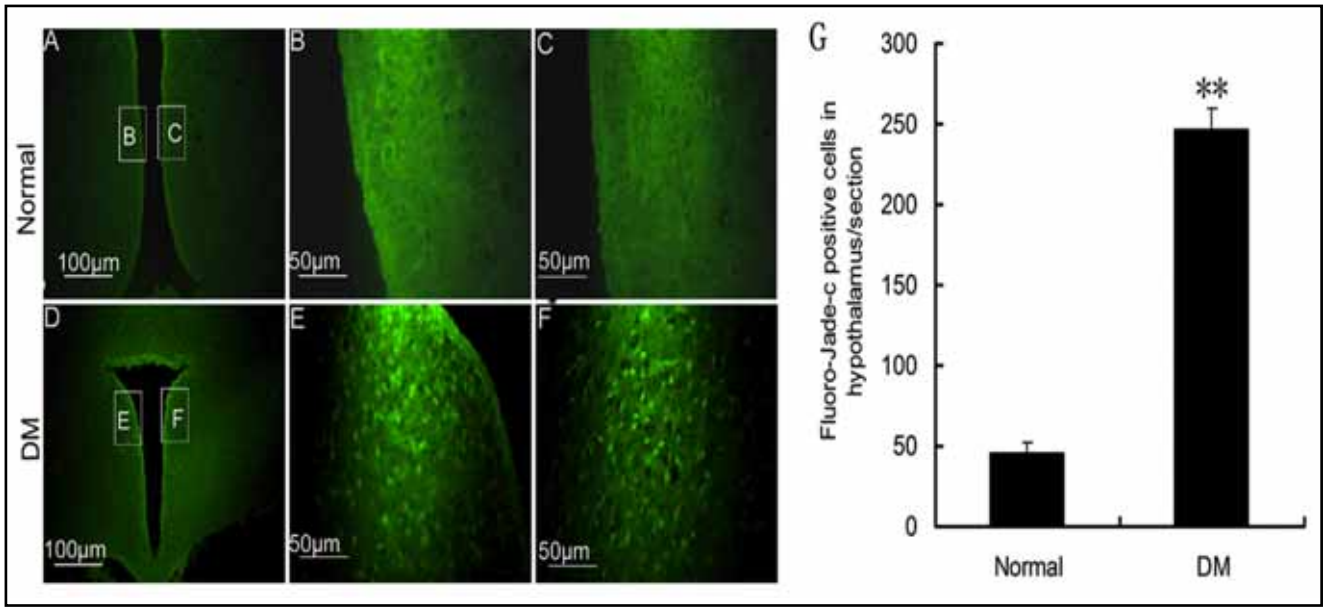

Fig. 3. Neuron damage in the hypothalamus of T2DM mice. (A–F), microphotographs of Fluoro-Jade C staining in the hypothalamus. (B and C), magnified images of the squares in (A). (E and F), magnified images of the squares in (D). (G), quantification of Fluoro-Jade C–positive cells in the hypothalamus. Data are expressed as mean ± SEM. n=6. ** $p<0.01$, mice treated with low-dose STZ combined with high-fat diet for 4 months vs normal mice.

Neuron degeneration in the hypothalamus of T2DM mice

FJC staining was performed to evaluate the neuron survival in the diabetic mice. As shown in Figures 3A to G, the number of FJC-positive neurons was higher in the hypothalamic ventromedial nucleus and arcuate nucleus of the diabetic mice than those of the normal mice. This result showed that neuron degeneration was markedly increased in the hypothalamus of the diabetic mice than that of the normal mice.

Changes of autophagic signals in the hypothalamus of diabetic mice

Insulin signals negatively regulate autophagy by activating the mTOR. Therefore, the changes in autophagic signals in the hypothalamus were further investigated in this study. As shown in Figures 4A and B, the level of phospho-mTOR increased in the hypothalamus of the diabetic mice, suggesting the activation of mTOR. LC3II, which was located downstream of the autophagy pathway, was also significantly decreased in the hypothalamus of the diabetic mice (Figures 4C and D). The autophagic morphology of the neurons from the hypothalamic arcuate nucleus was observed under an electron microscope. As shown in Figure 4E, the number of autophagosomes increased in the neurons from the hypothalamic arcuate nucleus of the diabetic mice than that of the normal mice.

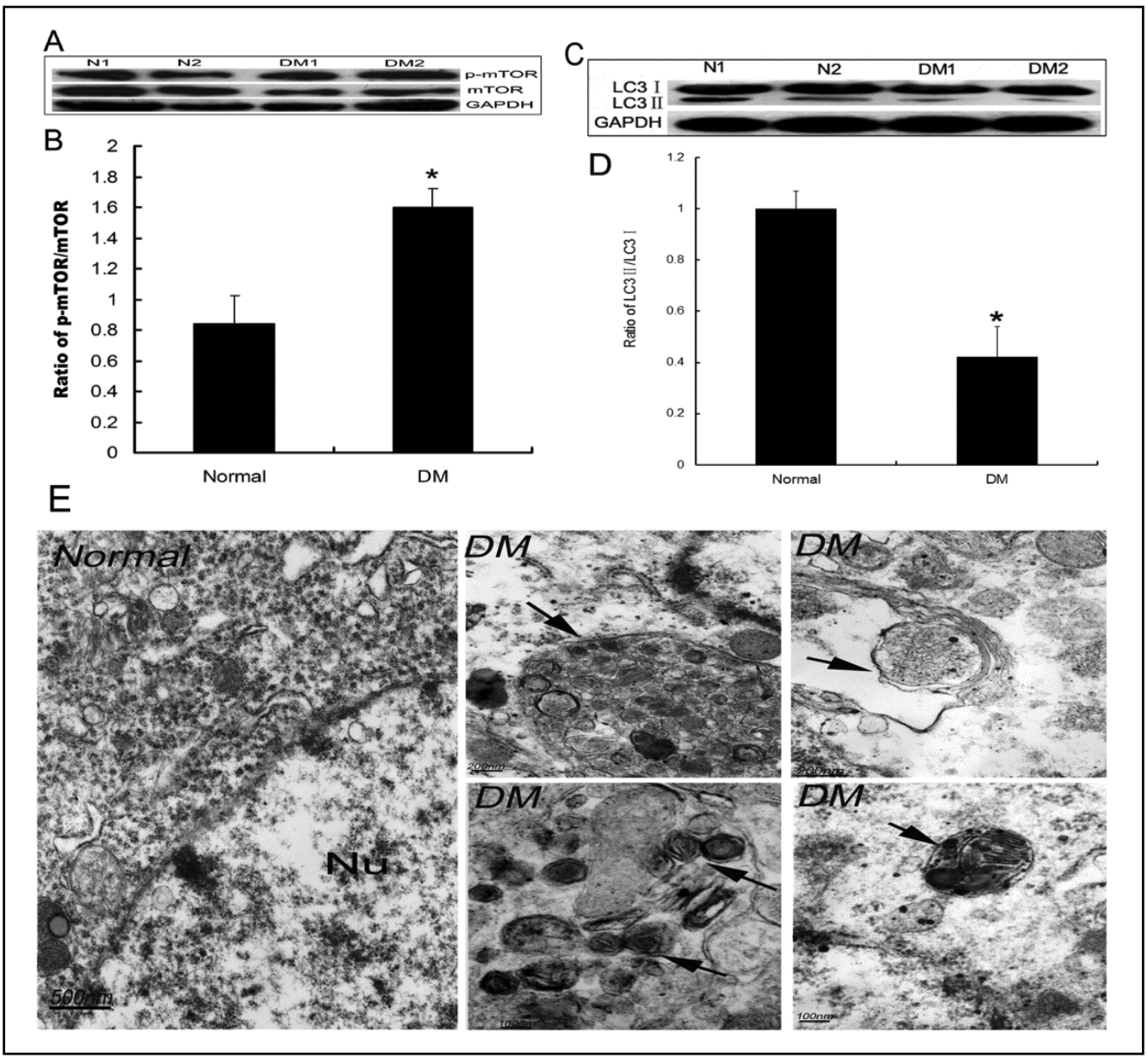

Fig. 4. Alterations in autophagic signals in the hypothalamus of T2DM mice. (A and C), protein expression levels of phospho-mTOR and LC3II in the hypothalamus were analyzed by western blot, respectively. The blot shown here is representative of five experiments. (B and D), quantification of the protein expression levels of phospho-mTOR and LC3II. Data are presented as mean ± SEM. n=5. * $p<0.05$, mice treated with low-dose STZ combined with high-fat diet for 4 months vs. untreated mice. (E), electron micrographs of autophagosomes in the neuron of hypothalamic arcuate nucleus. Nu: Nucleus. Autophagosome is represented by an arrow.

Effects of lipotoxicity on autophagy and cell viability in PC12 cells

The relationship between neuron survival and autophagy induced by lipotoxicity was investigated. PC12 cells were treated with 200, 300 and 400 μM oleic acid for 24 h to mimic lipotoxicity. As shown in Figures 5A, B and C, oleic acid upregulated LC3II expression and decreased PC12 cell viability in a dose-dependent manner.

Protective effect of autophagy activation elicited by lipotoxicity on PC12 cells

The function of autophagy activation in lipid toxic injury was studied. The autophagy inhibitor 3-MA and the autophagy inducer rapamycin were used to alter autophagy activity. Pretreatment of cells with 3-MA significantly downregulated LC3II expression and aggravated PC12 cell death induced by treatment with 300 μM oleic acid for 24 h (Figures 5D and E). By contrast, pretreatment of cells with rapamycin upregulated LC3 II expression (Figures 5F and G) and ameliorated PC12 cell death caused by treatment with 300 μM oleic acid for 24 h (Figure 5H).

Increased number of autolysosomes induced by lipotoxicity

Autophagosome–lysosome fusion initiates lysosome degradation in the late stage of autophagy. Autophagosomes fused with lysosomes can be stained by MDC. MDC/PI double staining was performed to identify the effect of oleic acid on the number of MDC-positive cells. 3-MA reduced the number of MDC-positive cells, whereas rapamycin increased the number of MDC-positive cells (Figures 6A and B).

DISCUSSION

Peripheral key molecules that regulate metabolism include insulin, leptin, and ghrelin. These molecules are targeted in the hypothalamus, which is the axis of neuroendocrine regulation. Hypothalamic neurons, such as NPY/Agrp, POMC, and orexin, can be activated through the response of the hypothalamus to these molecules; this activation affects food intake, sleep, and behavioral pattern (Lopaschuk *et al.* 2010). Abnormal food and water intake behavior caused by insulin deficiency or insulin resistance is also demonstrated by diabetic patients. Therefore, a relationship exists between the hypothalamus and diabetes. The results of our previous experiment showed that diabetes increases peripheral blood glucose, which is accompanied by elevated glucose level in the cerebrospinal fluid. In the present study, we found that insulin resistance induced by low-dose STZ combined with high-fat diet affected the hypothalamus. For example, downregulated IR and IRs1 expression and increased cholesterol content were observed in the hypothalamus. The mechanism underlying the increase in cholesterol level in the CNS is unclear, but it could be related to insulin signals and high blood glucose in the brain. Previous studies have established that cholesterol content in brain tissue is usually considerably higher than that in peripheral organs and that cholesterol is crucial in the composition of cell membrane and myelin sheath (Fukui *et al.* 2015). However, the effect of elevated cholesterol levels on the CNS remains controversial. Some studies have shown that an increase in cholesterol level in the nervous tissue of AD animal models enhances γ-secretase activity and accelerates Aβ42 aggregation (Kim *et al.* 2016). Moreover, elevated cholesterol in neuron mitochondria decreases antioxidant ability and increases cell sensitivity to Aβ42 damage (Raghavamenon *et al.* 2009). Apolipoprotein E, a vital molecule in lipid metabolism and polymorphisms, is the most pivotal susceptibility gene in AD onset (Zwan *et al.* 2015). This finding suggests that lipid metabolism has direct involvement in neuronal damage.

The most critical function of peripheral insulin signals is to regulate glucose metabolism. Insulin signals in the hypothalamus are involved in the regulation of feeding behavior. Insulin signals mediated by IRs are also closely related to neuron survival and activity-dependent synaptic plasticity (Tropea *et al.* 2006; Yao *et al.* 2012). For instance, adult hippocampal neural stem cells undergo autophagic cell death after insulin withdrawal (Yeo *et al.* 2016). Many studies have shown that insulin signals in the hypothalamus participate in the regulation of food intake. Third ventricle injections of insulin can inhibit feeding behavior in animals, whereas insulin deficiency promotes feeding behavior (Spencer, 2013). In the present study, the expression levels of IR and IRs1 were downregulated in the hypothalamus of the diabetic mice; this phenomenon was accompanied by increased feeding (data not shown). However, we found no direct evident to prove that low insulin signals in the hypothalamus cause neuronal damage.

mTOR is a vital molecule in autophagic negative control signals. The activity of mTOR can be negatively regulated by insulin signals through the PI3K-AKT/PKB pathway. In this study, the phosphorylation level and hence activity of mTOR increased in the hypothalamus of the diabetic mice. This increase could be a direct effect of insulin deficiency. mTOR not only negatively regulates autophagy; it also regulates feeding, synaptic plasticity, and memory formation (Bockaert and Marin, 2015). In this study, the phenomenon of autophagy under insulin deficiency was further studied. Western blot was performed to observe changes in LC3II expression in the hypothalamus of the diabetic mice. The results showed that LC3II expression was downregulated in the hypothalamus of the diabetic mice. Changes in autophagosome morphology were observed under an electron microscope to clarify the distribution of autophagosomes in the hypothalamic neuron. Autophagosome aggregation was significantly elevated in the neurons from the hypothalamic arcu-

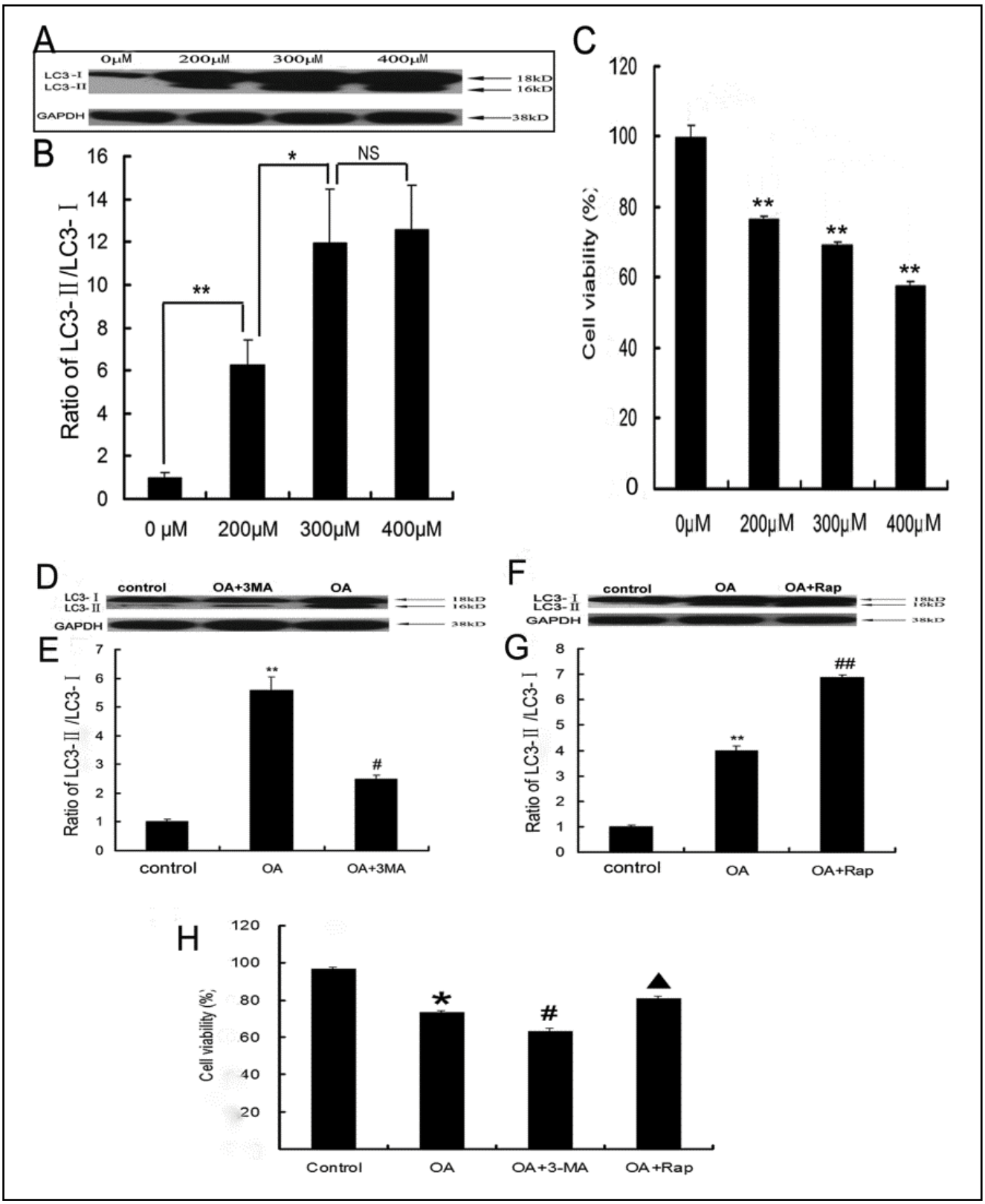

Fig. 5. Roles of autophagy in PC12 cells during incubation with oleic acid. (A), PC12 cells were treated with 200, 300 and 400 μM oleic acid for 24 h. Protein expression of LC3II in PC12 cells was analyzed by western blot. (B), quantification of the protein expression of LC3II. (C), PC12 cells were treated with 200, 300 and 400 μM oleic acid for 24 h. Cell viability was determined by the MTT assay and expressed as the percentage of untreated control. Data are presented as mean ± SD, n=3; * $p<0.01$, ** $p<0.01$ vs control group (no oleic acid incubation). (D and F), after 2 h treatment with 2.5 mM 3-MA or 2 μM rapamycin, PC12 cells were incubated with 300 μM oleic acid for 24 h. Protein expression of LC3II in PC12 cells was analyzed by western blot. (E and G), quantification of the protein expression of LC3II. (H) After 2 h treatment with 2.5 mM 3-MA or 2 μM rapamycin, PC12 cells were incubated with 300 μM oleic acid for 24 h. Cell viability was determined by the MTT method and expressed as the percentage of untreated control. Data are presented as mean ± SD. n=3. * $p<0.05$, ** $p<0.01$ vs control group. # $p<0.05$, ## $p<0.01$, ▲ $p<0.05$ vs OA group.

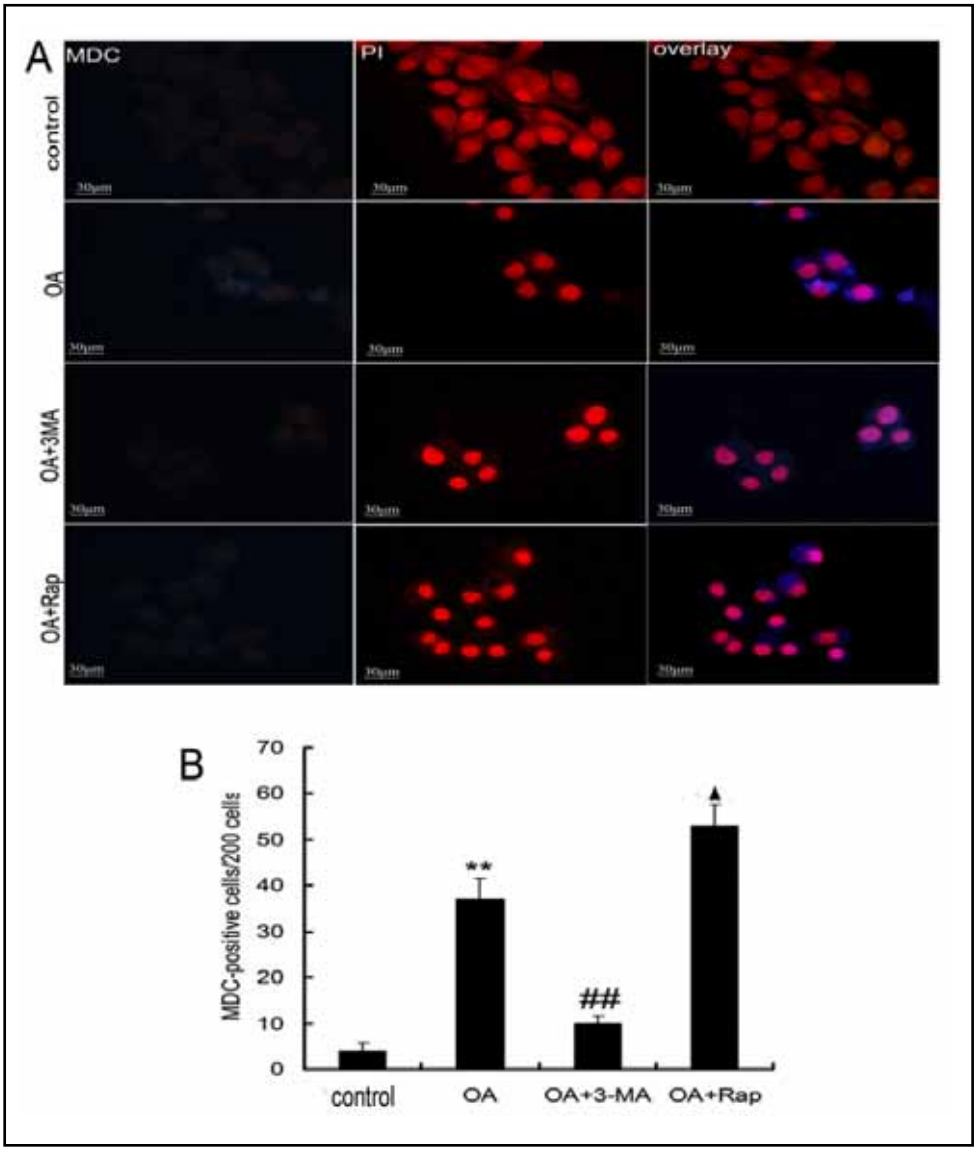

Fig. 6. Autophagy–lysosome fusion induced by incubation with oleic acid in PC12 cells. (A), after 2 h treatment with 2.5 mM 3-MA or 2 μM rapamycin, PC12 cells were incubated with 300 μM for 24 h. Autophagic vacuoles were observed by MDC incorporation assay under a fluorescence microscope. Representative photographs of MDC/PI double staining in PC12 cells. (B), quantification of MDC-positive cells according to the material and methods. ** $p<0.01$, cells were treated with oleic acid vs. untreated cells. ## $p<0.01$, cells were treated with 3-MA and oleic acid vs. treatment with oleic acid alone. ▲ $p<0.05$, cells were treated with rapamycin and oleic acid compared to the treatment with oleic acid alone.

ate nucleus of 4-month-old diabetic mice. Basing on the lower LC3II expression in the diabetic mice, we hypothesized that autophagosome degradation was failure. Generally, the half-life of autophagosomes is short. Therefore, little of autophagosome aggregation was observe in normal mice.

The hypothalamus of diabetic mice contains high cholesterol level, and PC12 cells are neuron-like cells. In the present study, PC12 cells were treated with oleic acid to mimic lipotoxicity. After oleic acid treatment, the viability of PC12 cells significantly decreased; this phenomenon was accompanied by autophagy activation. Autophagy activation is characterized by upregulated LC3II expression. PC12 cells were pretreated with 3-MA or rapamycin to identify the effects of autophagy activation caused by lipotoxicity in neurons. Autophagy activation elicited a protective effect on PC12 cells against lipotoxicity injury. MDC/PI double staining was performed to observe autophagosome–lysosome fusion induced by lipotoxicity. Autophagosomes can be fused with lysosome, suggesting that autophagosomes can be degraded.

In vivo, the insulin resistance was confirmed by insulin sensitivity assay and fast glucose tolerance test in diabetic mice in our present study (Figure 1). Further studies have been performed to observe the changes in hypothalamus which is the key area in regulation of metabolisms. Our dada indicated total cholesterol increased and expression of insulin receptor β (IRβ) and insulin receptor substrate 1 (IRs1) decreased in hypothalamus of diabetic mice compared to the control group. These results suggested insulin signal impaired in hypothalamus under the diabetic mellitus condition. Insulin deficit in hypothalamus partly contributed to the aberrant metabolism of lipid. Previous studies have been reported that insulin signal involved in regulation of autophagy (Williams 2013; Zhang *et al.* 2013; Riehle & Abel 2014; Liu *et al.* 2015a). In briefly, insulin bind-

ing to its receptor caused the phosphorylation of PI3K, which regulated the balance of the autophagy under the physiologic condition. But in insulin resistance condition, autophagy deficit characterized by accumulation of autophagosome contributed to the increase of mTOR phosphorylation. This is consistent with our results (Figure 4). To furtherly prove the function of autophagy under high lipid condition, PC12 cell lines were treated with oleic acid which is the main component of plasma lipid (Richieri & Kleinfeld 1995). The results indicated oleic acid induced activity of autophagy. But inhibition of autophagy with 3-MA, aggravated the cell damage following oleic acid treatment (Figure 5). These results suggested autophagy protected cells from oleic acid condition. Although treatment with oleic acid to PC12 cells only mimics the acute damage, future work needs to evaluate the level of autophagy under chronic high lipid conditions. Taken together, our present study aimed to prove the effects of periphery insulin resistance on central nervous system (especially, hypothalamus, the key region of metabolic regulation) *in vivo* and *in vitro*. The limitations of our experiment is that the downstream signal of insulin in hypothalamus was not studied under diabetic conditions, and did not observe whether the insulin signals in hypothalamus can be rescued through improving the lipid metabolisms.

In conclusion, the results from *in vivo* experiments showed that insulin signals were declined, autophagy was abnormal, and neuron damage was augmented in the hypothalamus of T2DM mice. And *in vitro*, results revealed that autophagy elicited a protective effect on PC12 cells against lipotoxicity. Autophagy activation might benefit energy utilization in neurons under stress conditions. Overall, these results suggest that autophagy activation confers protection to neurons in the early phase of the disorder under aberrant metabolism. These results also indicate that autophagy dysfunction in the hypothalamus occurs under the conditions of the chronic metabolic disorder, which leads to failure of autophagosome degradation.

ACKNOWLEDGEMENT

This work is partly supported by National Natural Science Foundation of China (No. 81370448 and 81570725) to Jing Yu Hong.

Declaration of interest

The authors declare no conflict of interests.

REFERENCES

1 Bernal-Reyes R (2012). [Fatty liver, alcoholic steatohepatitis, and non-alcoholic steatohepatitis] Revista de gastroenterologia de Mexico. **77 Suppl 1**: 84–86.
2 Biessels GJ, Reagan LP (2015). Hippocampal insulin resistance and cognitive dysfunction. Nat Rev Neurosci. **16**: 660–671.
3 Bockaert J, Marin P (2015). mTOR in Brain Physiology and Pathologies. Physiol Rev. **95**: 1157–1187.
4 Fukui K, Ferris HA, Kahn CR (2015). Effect of cholesterol reduction on receptor signaling in neurons. J Biol Chem. **290**: 26383–26392.
5 Gray SM, Meijer RI, Barrett EJ (2014). Insulin regulates brain function, but how does it get there? Diabetes. **63**: 3992–3997.
6 Haan MN (2006). Therapy Insight: type 2 diabetes mellitus and the risk of late-onset Alzheimer's disease. Nat Clin Pract Neurol. **2**: 159–166.
7 Hoyer S (2004). Causes and consequences of disturbances of cerebral glucose metabolism in sporadic Alzheimer disease: therapeutic implications. Advances in experimental medicine and biology. **541**: 135–152.
8 Iwangoff P, Armbruster R, Enz A, Meier-Ruge W (1980). Glycolytic enzymes from human autoptic brain cortex: normal aged and demented cases. Mechanisms of ageing and development. **14**: 203–209.
9 Kim Y, Kim C, Jang HY, Mook-Jung I (2016). Inhibition of Cholesterol Biosynthesis Reduces gamma-Secretase Activity and Amyloid-beta Generation. J Alzheimers Dis. **51**: 1057–1068.
10 Lee JH, Choi Y, Jun C, Hong YS, Cho HB, Kim JE, Lyoo IK (2014). Neurocognitive changes and their neural correlates in patients with type 2 diabetes mellitus. Endocrinol Metab (Seoul) **29**: 112–121.
11 Li L, Holscher C (2007). Common pathological processes in Alzheimer disease and type 2 diabetes: a review. Brain Res Rev. **56**: 384–402.
12 Ling D, Salvaterra PM (2009). A central role for autophagy in Alzheimer-type neurodegeneration. Autophagy. **5**: 738–740.
13 Liu J, Li H, Zhou B, Xu L, Kang X, Yang W, Wu S, Sun H (2015a). PGRN induces impaired insulin sensitivity and defective autophagy in hepatic insulin resistance. Mol Endocrinol. **29**: 528–541.
14 Liu X, Huang S, Wang X, Tang B, Li W, Mao Z (2015b). Chaperone-mediated autophagy and neurodegeneration: connections, mechanisms, and therapeutic implications. Neurosci Bull. **31**: 407–415.
15 Lopaschuk GD, Ussher JR, Jaswal JS (2010). Targeting intermediary metabolism in the hypothalamus as a mechanism to regulate appetite. Pharmacol Rev. **62**: 237–264.
16 Maiese K (2016). Targeting molecules to medicine with mTOR, autophagy, and neurodegenerative disorders. Br J Clin Pharmacol. **82**: 1245–1266.
17 Mizushima N (2005). The pleiotropic role of autophagy: from protein metabolism to bactericide. Cell Death Differ. **12 Suppl 2**: 1535–1541.
18 O'Farrell F, Rusten TE, Stenmark H (2013). Phosphoinositide 3-kinases as accelerators and brakes of autophagy. Febs J. **280**: 6322–6337.
19 Osellame LD, Duchen MR (2014). Quality control gone wrong: mitochondria, lysosomal storage disorders and neurodegeneration. Br J Pharmacol. **171**: 1958–1972.
20 Raghavamenon AC, Gernapudi R, Babu S, D'Auvergne O, Murthy SN, Kadowitz PJ, Uppu RM (2009). Intracellular oxidative stress and cytotoxicity in rat primary cortical neurons exposed to cholesterol secoaldehyde. Biochem Biophys Res Commun. **386**: 170–174.
21 Richieri GV, Kleinfeld AM (1995). Unbound free fatty acid levels in human serum. J Lipid Res. **36**: 229–240.
22 Riehle C, Abel ED (2014). Insulin regulation of myocardial autophagy. Circ J. **78**: 2569–2576.
23 Rivera EJ, Goldin A, Fulmer N, Tavares R, Wands JR, de la Monte SM (2005). Insulin and insulin-like growth factor expression and function deteriorate with progression of Alzheimer's disease: link to brain reductions in acetylcholine. J Alzheimers Dis. **8**: 247–268.
24 Rubinsztein DC, Gestwicki JE, Murphy LO, Klionsky DJ (2007). Potential therapeutic applications of autophagy. Nat Rev Drug Discov. **6**: 304–312.
25 Savage DB, Petersen KF, Shulman GI (2007). Disordered lipid metabolism and the pathogenesis of insulin resistance. Physiol Rev. **87**: 507–520.
26 Sims NR, Bowen DM, Smith CC, Flack RH, Davison AN, Snowden JS, Neary D (1980). Glucose metabolism and acetylcholine synthesis in relation to neuronal activity in Alzheimer's disease. Lancet (London, England). **1**: 333–336.

27 Spencer SJ (2013). Perinatal programming of neuroendocrine mechanisms connecting feeding behavior and stress. Front Neurosci. **7**: 109.
28 Steen E, Terry BM, Rivera EJ, Cannon JL, Neely TR, Tavares R, Xu XJ, Wands JR, de la Monte SM (2005). Impaired insulin and insulin-like growth factor expression and signaling mechanisms in Alzheimer's disease--is this type 3 diabetes? J Alzheimers Dis. **7**: 63–80.
29 Tropea D, Kreiman G, Lyckman A, Mukherjee S, Yu H, Horng S, Sur M (2006). Gene expression changesand molecular pathways mediating activity-dependent plasticity in visual cortex. Nat Neurosci. **9**: 660–668.
30 Tung YT, Wang BJ, Hu MK, Hsu WM, Lee H, Huang WP, Liao YF (2012). Autophagy: a double-edged sword in Alzheimer's disease. J Biosci. **37**: 157–165.
31 Williams LM (2013). Hypothalamic dysfunction in obesity. Proc Nutr Soc. **71**: 521–533.
32 Yang Y, Xu K, Koike T, Zheng X (2008). Transport of autophagosomes in neurites of PC12 cells during serum deprivation. Autophagy. **4**: 243–245.
33 Yao JJ, Gao XF, Chow CW, Zhan XQ, Hu CL, Mei YA (2012). Neuritin activates insulin receptor pathway to up-regulate Kv4.2-mediated transient outward K+ current in rat cerebellar granule neurons. J Biol Chem. **287**: 41534–41545.
34 Yeo BK, Hong CJ, Chung KM, Woo H, Kim K, Jung S, Kim EK, Yu SW (2016). Valosin-containing protein is a key mediator between autophagic cell death and apoptosis in adult hippocampal neural stem cells following insulin withdrawal. Mol Brain. **9**: 31.
35 Zhang DD, Yu HL, Ma WW, Liu QR, Han J, Wang H, Xiao R (2015). 27-Hydroxycholesterol contributes to disruptive effects on learning and memory by modulating cholesterol metabolism in the rat brain. Neuroscience. **300**: 163–173.
36 Zhang Y, Xu X, Ren J (2013). MTOR overactivation and interrupted autophagy flux in obese hearts: a dicey assembly? Autophagy. **9**: 939–941.
37 Zwan MD, Villemagne VL, Dore V, Buckley R, Bourgeat P, Veljanoski R, Salvado O, Williams R, Margison L, Rembach A, Macaulay SL, Martins R, Ames D, van der Flier WM, Ellis KA, Scheltens P, Masters CL, Rowe CC (2015). Subjective Memory Complaints in APOEvarepsilon4 Carriers are Associated with High Amyloid-beta Burden. J Alzheimers Dis. **49**: 1115–1122.